13th World Conference on Earthquake Engineering
Vancouver, B.C., Canada
August 1-6, 2004
Paper No. 1599

ANALYTICAL AND EXPERIMENTAL STUDIES ON SEISMIC BEHAVIOR OF DEEP COLUMN-TO-BEAM WELDED REDUCED BEAM SECTION MOMENT CONNECTIONS

Xiaofeng ZHANG[1], James M. RICLES[2], Le-Wu LU[3], John W. FISHER[4]

SUMMARY

An analytical and experimental study was conducted to investigate the seismic behavior of reduced beam section (RBS) moment connections to a deep wide flange column. Three-dimensional finite element models of RBS connections in perimeter moment resisting frames (MRFs) with deep columns were developed and used to perform parametric studies. The parameters in the analytical study included: column depth, panel zone strength, composite floor slab, and beam web slenderness. The test matrix for the experimental program consisted of six full-scale interior RBS connections, where the column for the specimens ranged in depth from W24 to W36. All but one of the specimens had a composite floor slab. The results from the parametric study show that a composite floor slab provides restraint to the top flange of the beams; reducing the magnitude of beam top and bottom flange lateral movement in the RBS, column twist, and strength degradation due to beam instability in the RBS. The performance of each of the test specimens was found to meet the seismic connection qualification criteria in Appendix S of the AISC Seismic Provisions, and thereby have sufficient ductility for seismic resistant design.

INTRODUCTION

RBS beam-to-column moment connections are often utilized in the design of special steel moment resistant frames (SMRFs). The details of a typical RBS connection are shown in Figure 1(a), where the flanges of the beam are reduced in width, away from the column face. CJP welds attach the beam flanges to the column. The beam web is often welded to the column flange with a CJP weld. By design, the RBS connection develops inelastic deformations primarily in the region where the beam flange width has been reduced (referred to herein as the RBS), limiting the inelastic strain developed in the beam flange-to-

[1] Graduate Research Assistant, Dept. of Civil Eng., Lehigh Univ., 117 ATLSS Dr. Bldg H, Bethlehem, Pa. 18015, U.S.A., xiz6@lehigh.edu
[2] Professor, Dept. of Civil Eng., Lehigh Univ., 117 ATLSS Dr. Bldg H, Bethlehem, Pa. 18015, U.S.A., jmr5@lehigh.edu
[3] Professor, Dept. of Civil Eng., Lehigh Univ., 117 ATLSS Dr. Bldg H, Bethlehem, Pa. 18015, U.S.A., lwl0@lehigh.edu
[4] Professor, Dept. of Civil Eng., Lehigh Univ., 117 ATLSS Dr. Bldg H, Bethlehem, Pa. 18015, U.S.A., jwf2@lehigh.edu

column CJP welds. With the reduction of the beam flange width, an RBS connection is more prone to inelastic local buckling of the beam web and flanges in the RBS. For economical reasons, design engineers in the U.S. prefer to use deep columns in SMRFs (as large as 914 mm in depth corresponding to a W36 wide flange section) in order to control seismic drift. Previous tests on RBS connections have been performed primarily on columns with depths corresponding to a W12 and W14 wide flange section (Roeder [1]), where the depth was about 305 mm to 356 mm. Some tests using W27 wide flange column sections (686 mm depth) were conducted by Chi and Uang [2], where the connection was an exterior connection (i.e., only one beam was connected to the column). It was observed in these tests, that as a result of inelastic beam web and flange local buckling in the RBS, a lateral displacement of the beam compression flanges occurs. Shown in Figure 1(b) is the movement of the compression flanges (the top and bottom flanges of the right and left-hand beams, respectively), where F_1 and F_2 represent the beam flange compression forces of the two beams. Due to an eccentricity created by the lateral movement of the compression flanges, a torque is applied to the column. Deep columns tend to have thinner flanges and a web than a shallower column, resulting in a reduced torsional resistance. Consequently, there have been concerns that the use of an RBS connection to a deep column in a MRF can lead to inferior seismic performance because of it being susceptibility to torsional loading from the beams.

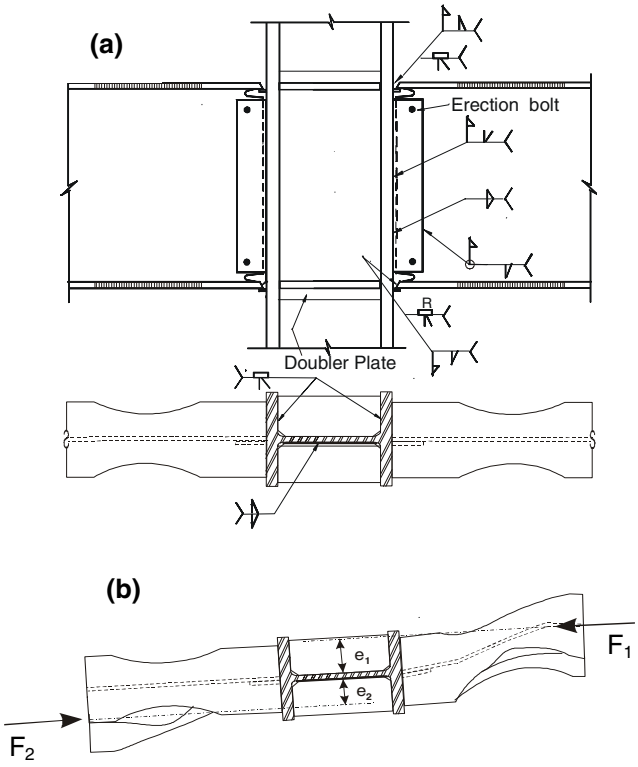

Figure 1. (a) RBS connection details, and (b) RBS local buckling and lateral beam flange movement.

The lack of knowledge of the performance of RBS beam-to-deep column connections under seismic loading led to a study on this topic at Lehigh University [3]. The study involved both finite element analysis and experimental tests, and focused on RBS connections to a deep column. The effects of the column depth, a composite floor slab, panel zone strength, beam web slenderness, and supplemental lateral bracing at the end of the RBS section were examined. Nonlinear finite element models were developed and utilized to perform a parametric study. Six full-scale specimens were subsequently tested involving different column and beam sizes, a composite floor slab and supplemental lateral bracing. Results and conclusions from the finite element analysis and experimental studies are presented in this paper.

ANALYTICAL STUDY

The analytical study involved developing finite element models of connection subassemblies for the purpose of evaluating the effect of the various parameters on connection behavior. Three-dimensional nonlinear finite element models were created using the ABAQUS computer program [4]. The geometry (i.e., member span lengths) and boundary conditions of the connection subassemblies were based on the test setup used in the experimental study. Grade 50 steel (which has a nominal yield stress of 345 MPa) was used for the beams, column, doubler plates and continuity plates. The member section sizes for the models in the analysis matrix were based on representing the range of anticipated member section sizes

for the test specimens. Furthermore, the beam section size was selected for each model to ensure a weak beam-strong column configuration, which is required by the AISC Seismic Provisions [5]. The parameters were studied by varying the details in a model to create various finite element models. Both monotonic and cyclic loading analyses were performed.

Description and Verification of Finite Element Model

Two types of models were developed, namely a *global model* and a *sub-model.* The global model was used to perform analysis of the connection subassembly in order to evaluate the global response, such as lateral load-story drift response and column twist-story drift response. The sub-model was utilized to perform a local analysis of the connection in the region of the beam tension flange. The mesh sizes for both the global and sub-models were based on considering computer limitations that constrained the maximum number of degrees of freedom in a model, the need for greater accuracy near the connection region, and mesh convergence. Geometric and material non-linearities were included in both models, where the geometric nonlinearities were accounted for using a finite strain and displacement formulation. A von Mises material with strain-hardening was used to account for material nonlinearities.

The global model consisted of a cruciform interior connection subassembly. A typical three-dimensional finite element global model of a connection subassembly is shown in Figure 2, where the column height and beam lengths are 3962 mm and 4496 mm, respectively. The entire beam and column sections were included in the global model in order to include asymmetry due to any imperfections in the model and local buckling. In the global model, the beams and the column, as well as the connection attachments (i.e., continuity plates, doubler plates and groove welds) were modeled using a four-node shell element with standard integration (element S4 in the ABAQUS element library). A shell element was used to model the members in lieu of a solid element, since a shell element is more capable of properly capturing the effects of local buckling. In some models, to reduce computational effort, a four-node shell element with reduced integration (element S4R in the ABAQUS element library) was used in the regions in the column where the results were not critical and the material remained elastic. Depending on the section sizes and connection details, the mesh for the various models had each a different number of elements, nodes, and degrees of freedom. The mesh for a typical global model (consisting of a W36x230 column and two W36x150 beams) had approximately a total of 3,600 elements and 3,820 nodes, resulting in 22,566 degrees of freedom.

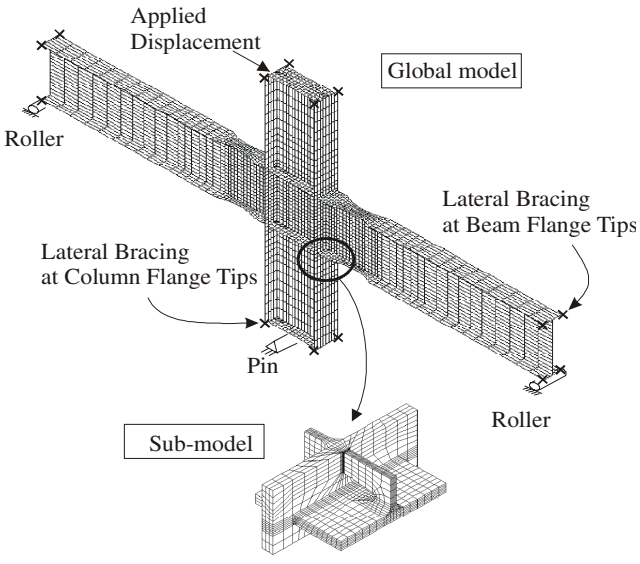

Figure 2. Finite element model (slab not shown for clarity).

The boundary conditions for a global model consisted of roller boundary conditions at the end of each beam as well as a pin boundary condition at the bottom of the column. The roller boundary condition allowed horizontal translation in the plane of the beam web and rotation about an axis that was normal to the plane of the beam web. In the pin boundary condition all displacements and rotation, except for the rotation about the axis normal to the plane of the connection, were restrained. Out-of-plane movement of the beam and column members was restrained at their flanges near the ends of the beams (at 4496 mm from column center line), and at the top and bottom of the column to simulate the lateral-torsional bracing for the test setup. For models with a composite floor slab, transverse floor beams at 3048 mm from the column centerline braced the

main beams, which is similar to how the specimens were braced in the setup. The distance of 3048 mm was based on the AISC Seismic Provisions [5] for bracing requirements for a W36x150 beam.

The area of interest in the connection analyses is primarily near the column-beam flange interface, where fracture may occur in either the weld metal or base metal near the beam flange CJP groove welds. The three-dimensional sub-models of the beam bottom flange-to-column flange connection region were generated to obtain more detailed and accurate information in order to evaluate the fracture potential in the connection region. The beam bottom flange was in tension under the monotonic loading imposed to the model (to be discussed later). These areas of a connection are deemed to be critical, and are identified in Figure 3.

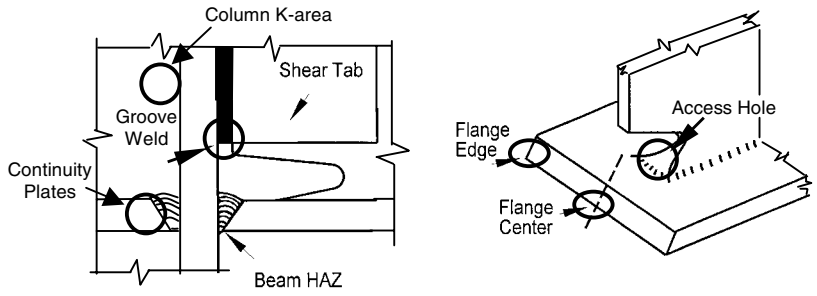

Figure 3. Critical regions in connection, beam tension flange.

The finite element model for a sub-model is included in Figure 2. The sub-models were composed of eight-node brick elements with standard integration (element C3D8 in the ABAQUS element library). The sub-model analysis directly utilized the results of the global model analysis as boundary conditions along the perimeter edges of the sub-model. Several sub-models were developed in order to accommodate the geometry of the beam and the different column section sizes and parameters in the study. The mesh for each model varied slightly in the number of elements, nodes, and degrees of freedom and was established through mesh convergence studies (to be discussed later). The mesh for a typical sub-model (W36x230 column and W36x150 beam) consisted of approximately 3,800 brick elements, 5,000 nodes, and 15,000 degrees of freedom. This sub-model had 18 elements and 6 elements through the width and thickness of the beam flange, respectively. Six elements were used through the thickness of the beam web and four elements through the thickness of the column flange.

The effects of the stiffness of column lateral and torsional bracing restraint were investigated in order to ensure that it did not influence the analysis results of the parametric study in such a way that they would not be representative of prototype member behavior. The results indicate that the column bracing is very important and that columns with a lack of torsional bracing have a reduction in strength and ductility of the subassembly due to excessive twist that resulted in yielding of the column. Excessively stiff torsional bracing does not significantly affect the results. Therefore the use of rollers to laterally and torsionally brace the ends of the column in the finite element models as well as in the test setup appears to be reasonable.

The composite floor slab was modeled using shell element type S4 in the ABAQUS element library along with an elastic-plastic compression-only stress material, while beam element type B33 (a two-node three-dimensional cubic formulation beam element) was used to model the transverse floor beams. The shear studs, which affix the composite floor slab to the main beams as well as the transverse floor beams, were modeled using spring element type SPRING2 in the ABAQUS element library. The spring elements were put in both horizontal directions, and displacement constraints were used in the vertical direction to avoid vertical separation between the beams and the floor slab. The shear stud model was based on that recommended by Lee and Lu [6]. The shear stud model was calibrated using the results from prior tests performed by Jones et al. [7] on specimens with composite floor slabs.

The finite element global model was verified by comparing the measured response of Specimen DBBWC tested by Jones et al. [7] with the response predicted by the finite element model. Specimen DBBWC consisted of an interior RBS connection, which was tested under Phase II of the SAC Steel Project using a cyclic inelastic loading protocol. The beams and columns for the specimen were W36x150 and W14x398 sections, respectively, fabricated from A572 grade 50 steel. The specimen had a composite floor slab that extended 1220 mm to both sides of the beam. The lateral load-story drift response predicted by the finite element model is compared to the test results in Figure 4. The response predicted by the model is in good agreement with the experimental results. The model properly predicted the occurrence of panel zone yielding, beam yielding, cyclic beam web and flange local buckling in the RBS, and strength deterioration that occurred in the test specimen. The comparison between the test and finite element analysis indicates that the finite element modeling procedures produce an accurate model, which should lead to accurate response prediction in the parametric study.

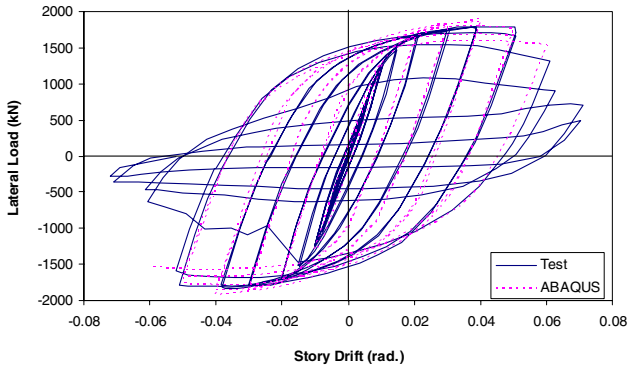

Figure 4. Results of validation study for finite element model.

Response Indices

To access the effect of the parameters on the ductile fracture potential of the models of the various connection configurations, the *Rupture Index (RI)* was computed from the finite element analysis results. The RI is defined as the ratio of the equivalent plastic strain *(PEEQ)* index to the ductile fracture strain ε_f, multiplied by the material constant α, i.e.

$$RI = \alpha \frac{PEEQ/\varepsilon_y}{\varepsilon_f} = \frac{PEEQ/\varepsilon_y}{\exp(1.5\frac{p}{q})} \tag{1}$$

where p and q are equal to the hydrostatic pressure and von Mises stress, respectively, with:

$$p = -\frac{1}{3}\text{trace}(\sigma_{ij}) = -\frac{1}{3}\sigma_{ii} \tag{2}$$

and

$$q = \sqrt{\frac{3}{2}S_{ij}S_{ij}} \tag{3}$$

The ratio of hydrostatic pressure-to-von Mises stress is known as the triaxiality ratio (TR), where larger negative values of this ratio lead to larger values of the RI (tension stress produces a negative hydrostatic pressure). The equivalent plastic strain is given as:

$$PEEQ = \sqrt{\frac{2}{3}\varepsilon_{ij}^{pl}\varepsilon_{ij}^{pl}} \tag{4}$$

Values of the RI were used to evaluate and compare the potential for ductile fracture of different locations in a finite element model or between two different models at the same location. Research by Hancock and Makenzie [8] has shown that this criterion for evaluating the potential for ductile fracture to be accurate.

Analysis Matrix

The analysis matrix for the finite element parametric study consists of 14 cases, which are summarized in Table 1. For each analysis case the following are identified: connection type (RBS vs. welded

unreinforced flange – WUF); column section size; beam section size; panel zone strength ratio R_v/V_{pz}, and whether a composite floor slab existed in the model. All cases consisted of a two-sided connection, except for Case 9 which had a one sided connection. R_v is the panel zone shear strength based on the AISC Seismic Provisions [5], as given below in Equation (5), while V_{pz} is the shear force in the panel zone corresponding to the maximum expected plastic moment M_{pr} [5] developing in the RBS based on Equation (6):

$$R_v = 0.6 F_y d_c t_p \left[1 + \frac{3 b_{cf} t_{cf}^2}{d_b d_c t_p} \right] \tag{5}$$

$$M_{pr} = C_{pr} R_y Z_{RBS} F_y \tag{6}$$

where F_y, d_c, t_p, b_{cf}, t_{cf}, and d_b are equal to the panel zone nominal yield strength, column depth, combined total thickness of the column web and doubler plate, column flange width, column flange thickness, and beam depth, respectively, and C_{pr}, R_y, Z_{RBS}, and F_y are equal to a factor to account for peak connection strength, ratio of expected yield strength of beam to minimum specified yield strength, plastic section modulus of the beam at the RBS section., and beam nominal yield strength.

The effects of beam web slenderness were investigated by considering 32 additional cases, all involving a two-sided RBS connection, both with and without a composite floor slab. 18 of these cases involved a W36x230 column section, with the beam section ranging in size from a W36x135 to a W36x256. The remaining 14 cases had a W27x194 column section, with the beam section ranging in size from a W36x135 to a W36x210.

Table 1. Analysis matrix.

Case	Conn. Type	Column	Beam	R_v/V_{pz}	Floor Slab
1	RBS	W14x398	W36x150	1.22	No
2	WUF	W14x398	W36x150	1.36	No
3	RBS	W36x230	W36x150	1.09	No
4	WUF	W36x230	W36x150	1.09	No
5	RBS	W27x194	W36x150	1.05	No
6	RBS	W36x230	W36x150	0.83	No
7	RBS	W36x230	W36x150	1.34	No
8	RBS	W27x146	W30x108	1.05	No
9	RBS	W27x194	W36x150	1.35	No
10	RBS	W14x398	W36x150	1.22	Yes
11	RBS	W36x230	W36x150	1.09	Yes
12	RBS	W27x194	W36x150	1.05	Yes
13	RBS	W27x194	W36x150	0.65	No
14	RBS	W27x194	W36x150	1.25	No

The analysis results for selected cases are given below, where they are grouped into two categories: *local performance*, and *global performance*. Local performance is related to the ductile fracture potential of the connection, as indicated by the value of the Rupture Index (RI). At the critical regions in the connection identified in Figure 3 the values for the RI were obtained from the analysis results for the finite element sub-model. The local performance and RI values were based on monotonic analyses with increasing displacements up to 6% story drift. The global performance is related to the cyclic behavior of the connection subassembly, where the effects of panel zone strength, column section size, composite floor slab, and beam web slenderness on the cyclic strength, lateral displacement of the beam compression flange in the RBS, and column twist were investigated. The cyclic displacement amplitude followed the loading protocol for cyclic qualification testing of beam-to-column moment connections given in Appendix S of the AISC Seismic Provisions [5].

Analysis Results

Local Performance

Effect of connection type - To examine the effect of connection type on ductile fracture potential, two types of connections, namely WUF and RBS, were investigated. Cases 1 and 2 in Table 1 both include a W14x398 section for the column. Cases 3 and 4 both have a deeper column section (W36x230). Case 5 had a deep column, but of smaller depth and weight (W27x194), with an RBS connection. The W27x194 section has the smallest torsional rigidity among the W36x230 and W14x398 sections. All of these cases had a W36x150 section for the beam, but did not have a floor slab.

The maximum values for the RI for the various critical regions in the connections for these cases are shown in Figure 5 at 4% story drift. Figure 5 indicates that the RBS connection has a lower RI, and thus fracture potential, compared to a WUF connection to a similar column section. The cause for the higher value of the RI in the WUF connection is due to the larger plastic strains that develop in the connection region near the column face. The maximum moment in the beam at the column face is smaller in the RBS connection than the WUF connection, where the latter has a considerable amount of strain hardening in the beam plastic hinge region. For most cases, the largest fracture potential is at the end of the beam web-to-column flange CJP groove weld. The larger value for the RI at this location and at the beam flange CJP groove weld for Case 5 is associated with a greater amount of local larger plastic strain that develops at these locations compared to the other cases.

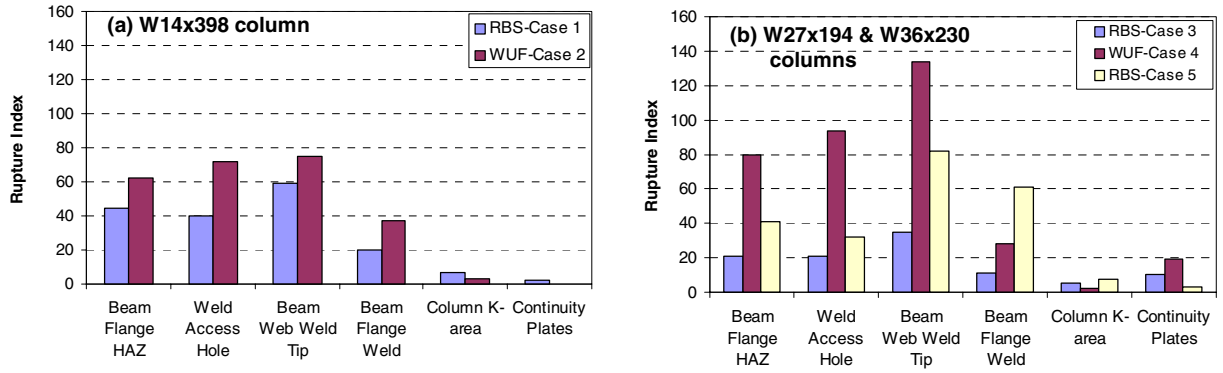

Figure 5. Effect of connection type on Rupture Index.

Effect of panel zone strength – The effect of panel zone strength on the ductile fracture potential of an RBS connection to a deep column was evaluated by comparing the results for Cases 3, 6, and 7. Each of these cases had a W36x230 column section and W36x150 beam section, but no composite floor slab. The values for the panel zone strength ratio R_y/V_{pz} are 1.09, 0.83, and 1.34 for Cases 3, 6, and 7, respectively. These values correspond to a *balanced panel zone strength* (with respect to the beam strength), *weak panel zone strength*, and *strong panel zone strength*. The thickness of the panel zone doubler plates corresponding to these strength conditions are 0, 6.4 mm, and 12.3 mm, respectively.

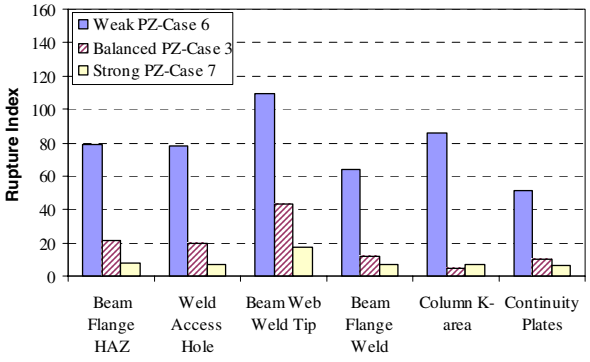

Figure 6. Effect of panel zone strength on Rupture Index, deep column RBS connection.

A summary of the maximum values of the RI at locations throughout the connection is given in Figure 6 at 4% story drift. It is apparent that a reduced panel zone strength results in an increase in the RI. The largest fracture potential is at the end of

the beam web-to-column flange CJP groove weld. The panel zone design based on current AISC Seismic Provisions [5], i.e., when R_t/V_{pz} is about equal to 1.0 (Case 3), shows a reduction in the RI by a factor of almost 2.0 throughout the connection compared to the case of a weak panel zone (Case 6) at 4% story drift. The strong panel zone design (Case 7) results in a further reduction in the RI, where at the end of the beam web CJP groove weld the reduction is by a factor of 6.0 compared to the weak panel zone case. The reason for this is because in the weak panel zone case, the panel zone underwent excessive plastic deformation and developed a large concentration of local plastic strain at the beam-to-column interface, particularly at the end of the beam web-to-column flange CJP groove weld. In the balanced panel zone case, the panel zone deformation was reduced, while in the strong panel zone case most of the plastic deformation develops in the RBS of the beam. The phenomenon of developing a large local plastic strain at the end of the beam web CJP groove weld in weaker panel zones was also found in studies by Ricles et al. [9] on WUF connections to W14 column sections.

Effect of column size - To evaluate the effect of the column section size on the performance of an RBS connection, five analysis cases involving different column sizes were performed. These cases included Cases 1, 3, 5, 8, and 9, which had column section sizes of W14x398, W36x230, W27x194, W27x146, and W27x194, respectively, where Case 9 has a one-sided RBS connection attached to a W27x194 column. For each of these cases, the beam size was selected to ensure a weak beam strong column configuration, and the panel zone was designed in accordance with ASIC Seismic Provisions [5], resulting in a balanced panel zone strength condition. No composite floor slab existed among these cases.

The values for the RI at the critical locations in the connection region are shown in Figure 7. The largest fracture potential is again at the end of the beam web-to-column flange CJP groove weld. The values of the RI are smallest in the column k-area and continuity plates. Case 5 is seen to have the largest value for the RI, which is due to the larger plastic strain that develops in the connection at the beam web weld. Although the W27x146 column section for Case 8 has a smaller section modulus and torsional resistance that the W27x194 column section for Case 5, the RBS connection to the W27x146 involves a smaller beam section (W30x108). Consequently, the strength demand on the connection is less in Case 8, as are the local plastic strains in the column flange and at the beam-column interface. The one-sided RBS connection, Case 9, is seen to have a lower value for the RI compared to Case 5, which has similar section sizes but is a two-sided RBS connection.

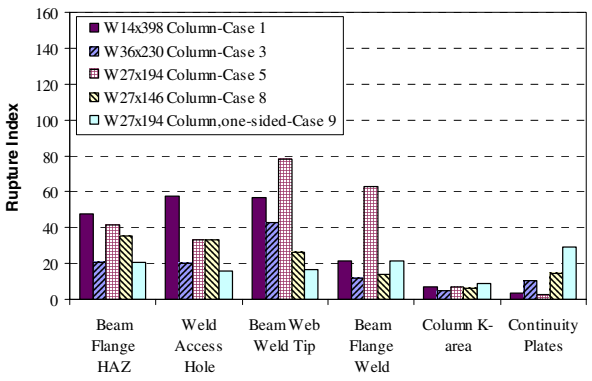

Figure 7. Effect of column section size on Rupture Index.

The results in Figure 7 indicate that the fracture potential does not necessarily increase in an RBS connection to a deeper column. Rather, the fracture potential of an RBS connection is highly dependent on the plastic strain that develops at the beam-column interface. For a given beam section size, a deeper column with a larger section modulus will have a lower fracture potential than one with a smaller section modulus, since in the former case the flexural and torsional warping normal stresses are smaller, leading to smaller local plastic deformations at the beam-column interface. Smaller beams can reduce the fracture potential of the connection by imposing smaller forces on the connection and column, leading to reduced plastic deformations in the connection.

Effect of composite floor slab - The effect of a composite floor slab on the ductile fracture potential of an RBS interior connection was investigated by performing the six analysis cases identified as Cases 1, 10, 3, 11, 5, and 12. The two parameters varied in the analysis matrix for these cases included the column section size and the presence of the floor slab. All of these cases have a W36x150 beam. Cases 1 and 10 have a W14x398 column without and with a floor slab, respectively, while Cases 3 and 11 have a W36x230 column without and with a floor slab, respectively. Cases 5 and 12 have a W27x194 column without and with a floor slab, respectively.

The results for the values of the RI at the connection are shown in Figures 8 and 9 for selected cases at 4% story drift. The floor slab is shown to increase the RI in all cases, where the maximum RI value for all cases occurs at the beam web-to-column-flange CJP groove weld. The increase in the RI at this location when adding a floor slab to the RBS connection having a W14x398 column (Case 10) is by a factor of two and due to an increase in both the local plastic strain (by a factor of two) and the triaxiality ratio TR (by 25%). For the deeper columns, the increase in the RI at this location when adding the slab is less, and equal to 47% for the W36x230 column (Case 3 vs. Case 11, not shown) and about 9% for the W27x194 column (Case 5 vs. Case 12). This modest increase in the RI for the RBS connections with a deeper column is due to the increase in the local plastic strain at the column-beam interface, with the triaxiality ratio TR not being affected as much by the presence of the floor slab. The larger section modulus for the deeper columns results in a smaller increase in plastic strain and triaxiality when the floor slab is added.

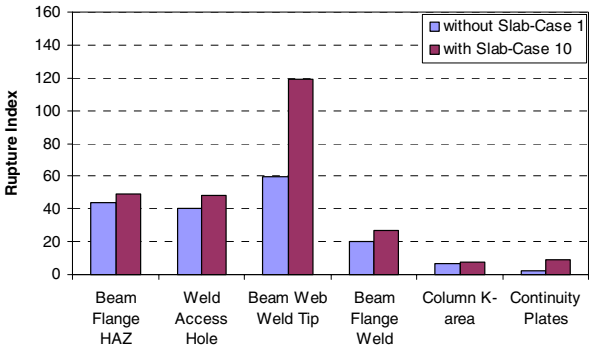

Figure 8. Effect of composite floor slab, W14x398 column.

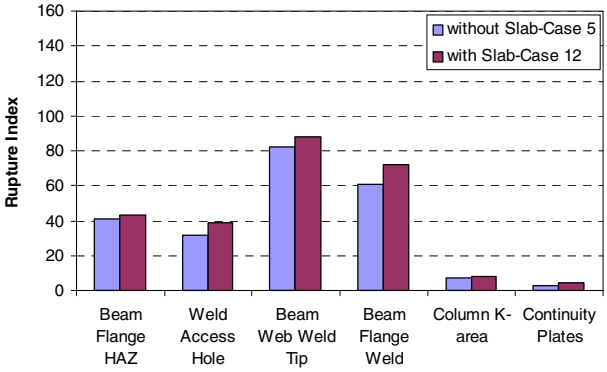

Figure 9. Effect of composite floor slab, W27x194 column.

Global Performance

Effect of panel zone strength - The effect of panel zone strength on the cyclic behavior of an RBS connection was investigated by performing three analysis cases. The analysis included one column size (W27x194) and three different panel zone strengths R_v corresponding to a weak panel zone (Case 13, R_v/V_{pz} = 0.65), a balanced panel zone (Case 5, R_v/V_{pz} = 1.05) and a strong panel zone (Case 14, R_v/V_{pz} = 1.25), respectively. The thickness of the doubler plate to achieve the different panel zone strengths for these cases was 0, 12.5 mm and 19 mm. The section size for the beams in all cases was a W36x150. None of these cases had a floor slab. The W27x194 section was selected for the study on global behavior, in lieu of the W36x320 section used in the study of the effect of panel zone strength on ductile fracture potential, because it was found that the W27x194 is more affected by panel zone strength.

The lateral load-story drift hysteretic response for all three cases is shown plotted in Figure 10. The hysteretic response has the weak panel zone (Case 13) developing the lowest strength, but not degrade in capacity, while the balanced and strong panel zone cases (Cases 5 and 14, respectively) have a deterioration in capacity due to beam local web and flange buckling, as well as lateral compression flange movement in the RBS. The deterioration in capacity commenced between 2% to 3% story drift. The

balanced and strong panel zone cases show an almost identical lateral load-story drift hysteretic response. The weak panel zone design had yielding and plastic deformations concentrated in the panel zone, leading to cyclic local buckling in the panel zone.

The column twist for all three cases at various story drifts is given in Figure 11. The weak panel zone case (Case 13) is shown to have minimal column twist, with significantly more twist developing in the models with a balanced and strong panel zone (Cases 5 and 14, respectively). The reason for this is because in the weak panel zone case the RBS did not develop significant yielding that would cause local buckling in the RBS. In the other two cases significant inelastic deformations developed in the RBS, leading to local buckling in the RBS and lateral beam compression flange movement, resulting in torsional loading and twisting of the column.

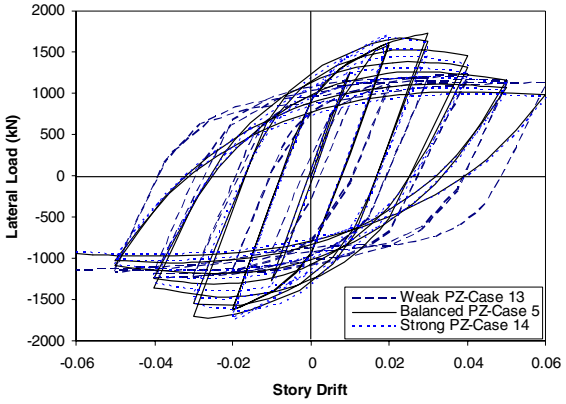

Figure 10. Effect of panel zone strength on cyclic strength.

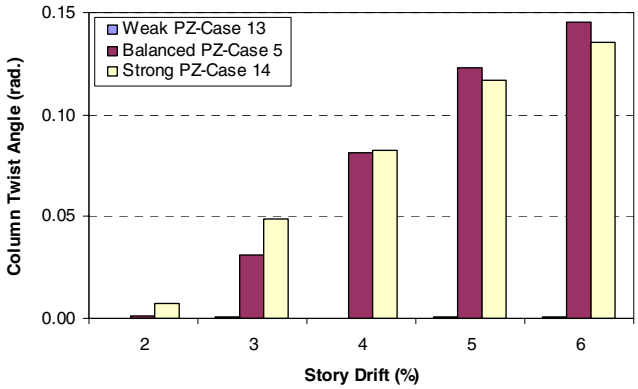

Figure 11. Effect of panel zone strength on maximum column twist.

Effect of composite floor slab and column section size- To investigate the effects of a composite floor slab and column section size on the global performance of an RBS connection, models with a bare steel connection and with a composite floor slab were both analyzed and their results compared. The same analysis cases used for investigating the effects of a composite floor slab on local performance were used to investigate global performance, namely, Cases 1 and 10, 3 and 11, and 5 and 12.

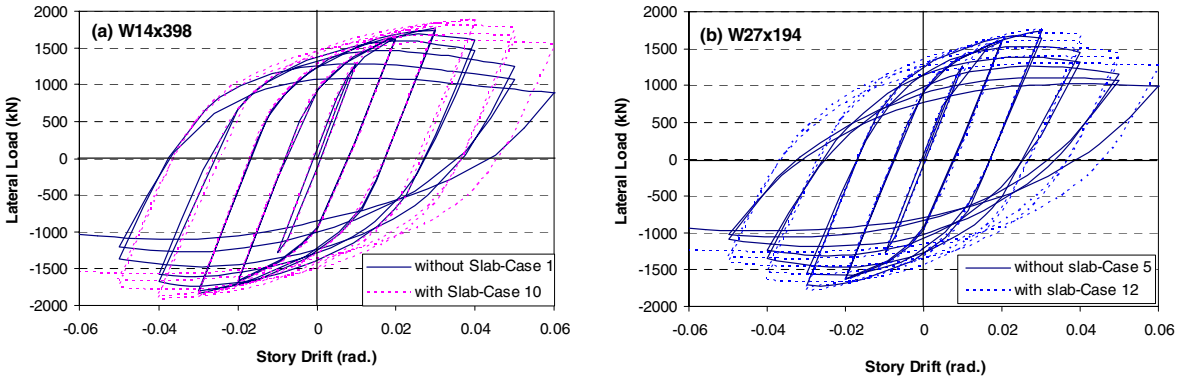

Figure 12. Effect of composite floor slab and column section on hysteretic behavior

The lateral load- story drift hysteretic response for Cases 1 and 10, and 5 and 12 is given in Figure 12. Cases with the same column section size are superimposed in Figures 12(a) and (b), respectively. It is apparent in Figure 12(a) and (b) that the floor slab enhances the performance of an RBS connection to

both a shallow and deep column by stabilizing the beam in the RBS region. The floor slab increases the strength of the connection, delays the onset of strength degradation, and reduces the amount of strength degradation. The floor slab has more of an effect on a connection to a shallower column section (Case 10, W14x398 column) compared to a deeper W27x194 column section (Case 12), where in the former case there is a greater increase in the strength and a reduction in the amount of strength degradation of an RBS connection. The increase in the maximum strength provided by the floor slab in these two cases is 4% and 2%, respectively. The extent of strength deterioration can be evaluated by comparing the response following local beam buckling that occurred at 3% story drift. At 4% story drift there is an 18% and 16% increase in strength for Cases 10 and 12, respectively, compared to their corresponding bare steel models. The enhancement of the connection performance (i.e., reduction in the amount of strength degradation) is consistent with the findings in the study by Jones et al. [7] on RBS connections to W14 column sections, who observed that the slab appears to have a stabilizing effect on the RBS moment connection, increasing the load and rotation capacity of the specimen.

Figure 13 shows the column twist angle at selected story drift levels for the same four cases. The results show a greater column twist for a deeper column (i.e., Cases 5 and 12), and a significant reduction in the column twist with the addition of the floor slab.

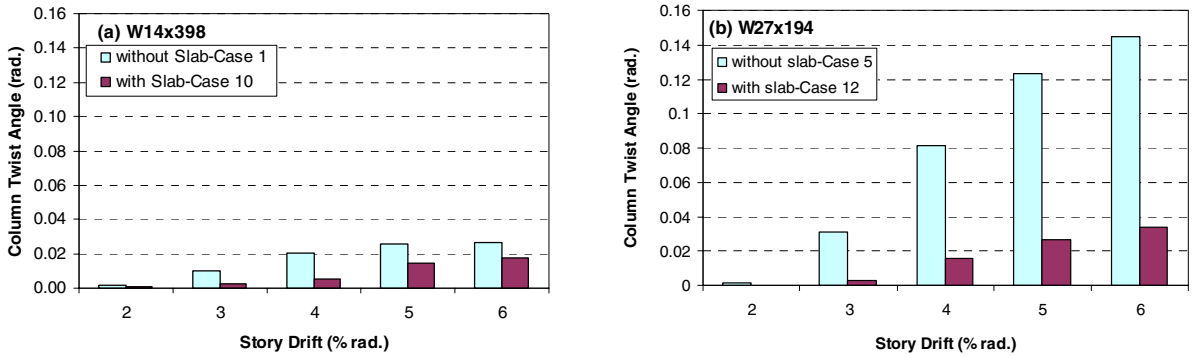

Figure 13. Effect of composite floor slab and column section on maximum column twist.

The column twist at 4% story drift for all six cases is plotted in Figure 14 against the column elastic torsional stiffness, considering both warping and St. Venant torsion effects. The appreciable reduction in column twist when adding a slab to the models is apparent. The trend in the relationship between column twist and column elastic torsional stiffness for cases with a floor slab is a straight line, implying that the column is behaving elastically in a global sense. A localized flange yielding occurred in the model with a W27x194 column section without a floor slab (Case 5), which led to an increase in the RI and the column twist and a deviation from a linear response is shown in Figure 14.

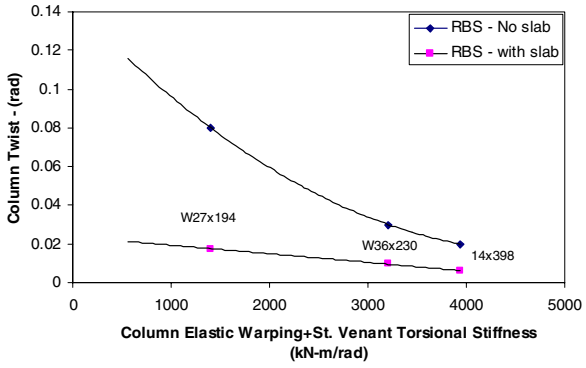

Figure 14. Effect of composite floor slab on column twist-elastic torsional stiffness.

Effect of beam web slenderness - The effect of beam web slenderness on the behavior of an RBS connection to a deep column was investigated by considering the 32 analyses mentioned previously. The

parameters in the analysis matrix consisted of beam web slenderness (W36 sections ranging in weight from 201 kg/m to 381 kg/m), column section size (W36x230 and W27x194), and the floor slab. The proportioning of the beam and column sizes in all of the analysis cases satisfied the weak beam-strong column criteria in the AISC Seismic Provisions [5].

The lateral (i.e., out-of-plane) movement of the beam bottom flange at the RBS is plotted as a function of the beam web slenderness in Figure 15 at 4% story drift. The results from the analysis show that the movement of the beam flange increases with a reduction in beam web slenderness for the cases without a floor slab. Furthermore, cases with a W27x194 column develop more beam flange movement in the RBS than those with a W36x230 column. The reason for this is associated with the lower column torsional flexibility and greater yielding that occurs in the cases involving the W27x194 column. The addition of the floor slab is shown to significantly decrease the transverse movement of the beam flange at the RBS, where the transverse movement is less than the value of $0.2b_f$, (b_f is the beam flange width), suggested by Chi and Uang [2] in their design procedure for RBS connections to a deep column.

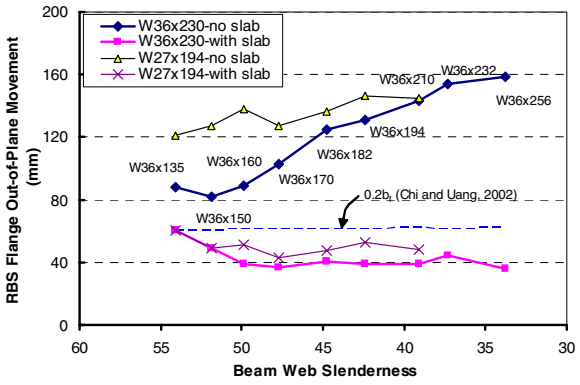

Figure 15. Effect of beam web slenderness on maximum RBS transverse movement, 4% story drift.

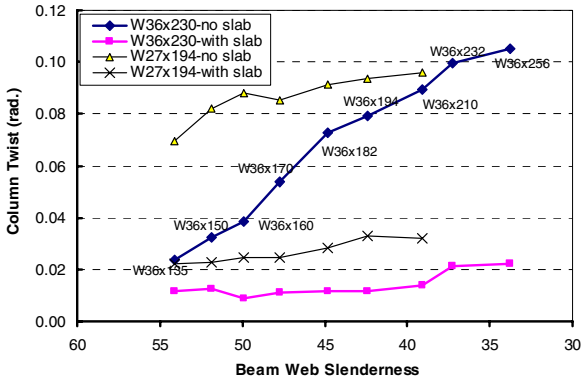

Figure 16. Effect of beam web slenderness on maximum column twist, 4% story drift.

The increase in the beam flange transverse movement of an RBS connection without a floor slab and reduced beam web slenderness is due to the effect of an increase in beam flange force. In the AISC Manual [10] the area of the beam flange increases in wide flange sections as the beam web slenderness is reduced. A larger beam flange area results in a larger flange compressive force, leading to a greater amount of torque applied to the column by the RBS connection.

The column twist developed in the models at 4% story drift is plotted against beam web slenderness in Figure 16. It is apparent in Figure 16 that the increase in beam flange area offsets the reduction in beam web slenderness, leading to an increase in column twist. Because the W27x194 is more flexible in torsion compared to the W36x230 section, for the same beam section the RBS connection to the W27x194 column results in a greater amount of column twist. The composite floor slab is shown to cause a significant reduction in the column twist, with an almost constant value compared to the results without a floor slab. Similar to the results in Figure 14, Figure 16 shows that the column twist for cases involving the W27x194 section is slightly more than that involving a W36x230 section when the floor slab is present.

In summary, the restraint provided to the beam top flange in the RBS results in the column twist not being sensitive to the beam web slenderness, and significantly reduces the beam bottom flange movement compared to results from models without the floor slab. The column torsional rigidity appears to be the main variable affecting column twist when a composite floor slab is present.

EXPERIMENTAL STUDY

Test Matrix

The experimental program involved the testing of six full-scale RBS beam-to-deep column connection specimens. The test matrix is given in Table 2. All specimens represented an interior RBS connection in a perimeter MRF with a composite floor slab, with the exception of SPEC-6 which did not have a composite floor slab. The parameters investigated in the experimental program included: (1) column size; (3) beam size; (4) the floor slab; and (5) supplemental lateral brace at the end of the RBS.

Table 2. Test matrix.

SPEC[(1)]	Column size	Beam Size	Floor Slab	Supp. Lat. Brace @ RBS	$K_{\phi,col}$ (kN-m/rad)	Col. Twist[(1)] (rad)	δ_{flg} RBS[(1)] (mm)	$0.2b_f$ (mm)
1	W36x230	W36x150	Yes	No	3190	0.016	53	61
2	W27x194	W36x150	Yes	No	1404	0.025	34	61
3	W27x194	W36x150	Yes	Yes	1404	0.006	35	-[(2)]
4	W36x150	W36x150	Yes	No	947	0.037	38	61
5	W27x146	W30x108	Yes	No	900	0.007	26	53
6	W24x131	W30x108	No	Yes	577	0.004	5	-[(2)]

Notes: (1) Corresponding to 4% story drift

(2) Chi and Uang [2] criteria for transverse beam flange movement does not apply to cases with supplemental braces

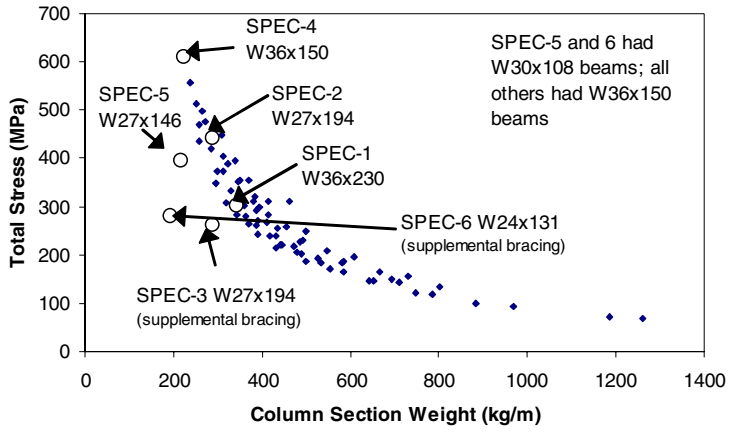

Figure 17. Column total stress per Chi and Uang [2] vesus column section weight.

The beam and column section sizes for each specimen were selected on the basis of introducing different degrees of torsional effects, predicted by the recommended design procedure by Chi and Uang [2], while also satisfying the weak beam-strong column criteria in the ASIC Seismic Provisions [5]. The design procedure by Chi and Uang considers the total normal stress in the column at 4% story drift due to axial load, flexure load, and torsion. The predicted total normal stress in the column flange is shown plotted in Figure 17 for various column sections, including those of the test specimens. Figure 17 indicates that SPEC-2, SPEC-4, and SPEC-5 are predicted to develop column flange yielding. The columns for all specimens and the beams for SPEC-3 through SPEC-6 were fabricated from A992 steel. The beams for SPEC-1 and SPEC-2 were fabricated from A572 Gr. 50 steel. Both A992 and A572 Gr. 50 have a nominal yield strength of 345 MPa.

Connection and Composite Floor Slab Details

The elevation of a typical connection detail is shown in Figure 18. Each specimen was designed in accordance with the criteria recommended by Engelhardt [11] for RBS connections, where the extrapolation of the beam moment in the RBS to the column face was limited to a value of $1.32M_{pn}$, where M_{pn} is the nominal plastic capacity of the beam. The reduction in flange width at the center of the RBS for each specimen was 50% of the original flange width, which complied with the design criteria by Engelhardt. The RBS was flame cut, with the burned surface ground to a surface roughness of 500 micro-inches, as recommended by FEMA 353 [12]. Each specimen had continuity plates the same thickness as the beam flanges and designed for a balanced panel zone design condition. Complete details are given in Ricles et al. [3]. The weld procedure specifications used in fabrication of the connections were prequalified in accordance with AWS D1.1/D1.1M:2002 [13]. All welds were done using the flux core arc welding procedure, and conformed to the AWS 5.20-95 Specification [14]. The beam flange-to-column flange CJP groove field welds and beam web-to-column CJP groove field welds utilized E70T-6 and E71T-8 electrodes, respectively. All shop welds (e.g., shear tab to the column, doubler and continuity plates) were performed using E70T-1. The run off tabs for the beam flanges were removed following the placement of the CJP groove welds, and the weld at the edges of the beam flanges ground to a smooth transition. The backing bar of the top flange weld was left in place and a reinforcement fillet weld was provided between the bottom surface of the backing bar and the column flange using the E71T-8 electrode. The beam bottom flange backing bar was removed using the air-arc process, back gouged, and reinforced with a fillet weld using an E71T-8 electrode. No run off tabs were used for the vertical beam web CJP groove welds. All CJP groove welds were inspected using the ultrasonic test procedure in order to evaluate whether they complied with the criteria in AWS D1.1 [13] for weld quality.

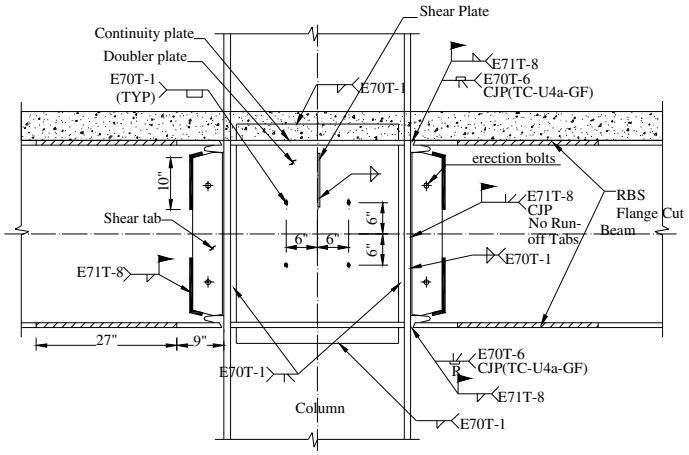

Figure 18. Specimen typical connection details (Note: 1 inch = 25.4 mm).

The specimen composite floor slab had a total thickness of 133 mm, and consisted of 27.6 MPa nominal compressive strength concrete cast on a 20-gage zinc coated metal deck. A W4x4 welded wire mesh with wire 152 mm on center was placed in the floor slab prior to pouring the concrete. The width of the floor slab was 1220 mm to one side, with a 305 mm overhang on the other side to simulate the conditions for a perimeter SMRF. The ribs of the decking ran parallel to the main beam of each test specimen. To develop the composite action, 19 mm diameter shear studs were placed outside the RBS region at 305 mm spacing along the beams to attach the deck to the main beams as well as transverse W14x22 floor beams. These transverse beams were placed at a spacing of 3048 mm to provide lateral bracing to the main beams and column, where the distance of 3048 mm satisfied the AISC Seismic Provisions [5].

SPEC-6, which had no composite floor slab, had a supplemental lateral brace at the end of the RBS in addition to the other lateral bracing for the beams. The lateral bracing was attached to a W36x150 section that was placed parallel to the beams of the test specimen to simulate a parallel beam in the prototype building. This parallel beam in the test setup was allowed to move horizontally with the test specimen, but restrained from out-of-plane movement. The corresponding stiffness of the lateral bracing setup satisfied

the AISC LRFD Specification [10]. SPEC-3 also had supplemental lateral braces, but these were anchored in the floor slab.

Test Setup, Loading Protocol, Instrumentation

The test setup is shown in Figure 19 (a), with the lateral bracing detail given in Figure 19(b) for the main beams. The ends of the members in the test setup had pin-connected boundary conditions using cylindrical bearings to simulate inflection points in the prototype frame. The ends of each beam away from the column were supported by instrumented rigid links, which simulated a roller boundary condition and enabled horizontal movement of the end of each beam. The lateral bracing detail shown in Figure 19(b) was used to prevent out-of-plane movement of the beams and column (the diagonal double angles were not used at the column), and designed for strength and stiffness in accordance with the AISC LRFD Specification [10]. The top of the column was braced against torsion, while at the base of the column a clevis was used to create the pin boundary condition. The beams were also braced at the rigid links in order to stabilize the test setup. The torsional bracing provided at both ends of the column was evaluated using the finite element model described previously to examine whether the stiffness would be representative of the torsional restraint at the column inflection points in the prototype structure. It was found to be satisfactory and not influence the test results by over-restraining the ends of the column from twisting.

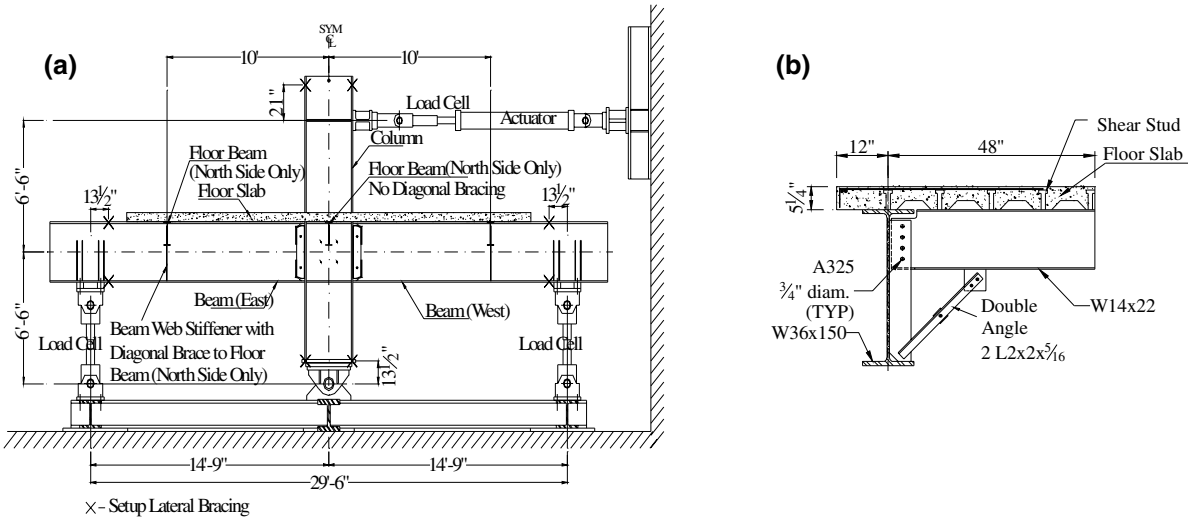

Figure 19. (a) Test setup and (b) beam lateral bracing detail for specimens with a composite floor slab (Note: 1 inch = 25.4 mm).

The specimens were tested by imposing a cyclic story drift history based on the loading sequence defined in Appendix S of the AISC Seismic Provisions [5]. The loading protocol consisted of initial elastic cycles of story drift, followed by cycles of increased amplitude to cause inelastic response. A test was terminated when either a fracture occurred, resulting in a significant loss of specimen capacity, or after reaching a story drift of 6%.

Each specimen was instrumented to enable measurement of the applied loads, reactions at the rigid links, specimen story drift; strains in the beam, column, panel zone, and continuity plates; in addition to panel zone deformation, plastic beam rotation, twisting of the column, and lateral displacement of the beam at the center of the RBS.

Test Results

Typical observed behavior during the testing of a specimen consisted of yielding in the RBS and the panel zone, followed by cyclic local web and flange buckling in the RBS. Following the development of local bucking in the RBS, lateral movement of the bottom beam flange began to occur in the RBS of specimens with a composite floor slab at 2% to 3% story drift. The combined effect of cyclic local buckling and lateral flange displacement resulted in a gradual deterioration in specimen capacity during subsequent cycles where the story drift amplitude was increased. This is evident in the lateral load-story drift hysteretic response of SPEC-4 shown in Figure 20. The lateral displacement of the bottom beam flange occurred when it was in compression, and caused some column twist to develop. The maximum column twist among the specimens with a floor slab at 4% story drift was 0.037 rads. (SPEC-4). 4% story drift is the drift at which connections are judged for qualification for seismic use by the AISC Seismic Provisions [5]. SPEC-4, like the other specimens, developed a flange fracture in the RBS where extensive local flange buckling had occurred. The local buckling in the beam flange led to large strains, resulting in a low cycle fatigue failure in the local buckled material. SPEC-6, which had a supplemental brace and lateral bracing attached to the beam that is parallel to the test beam, had minimal deterioration in capacity as well as column twist (0.004 rads. at 4% story drift). This was due to the restraint against lateral movement of the beam compression flange in the RBS, as well as the axial restraint by the parallel beam (which anchored the lateral bracing) against shortening of the test beam in the RBS following the onset of local buckling in the RBS. The measured longitudinal strains across the column flange just below the connection are shown in Figure 21 for SPEC-4 and SPEC-6. These results are representative of typical specimen behavior, and show little evidence of a strain gradient across the flange that would result from the effects of warping normal stresses due to column torsion.

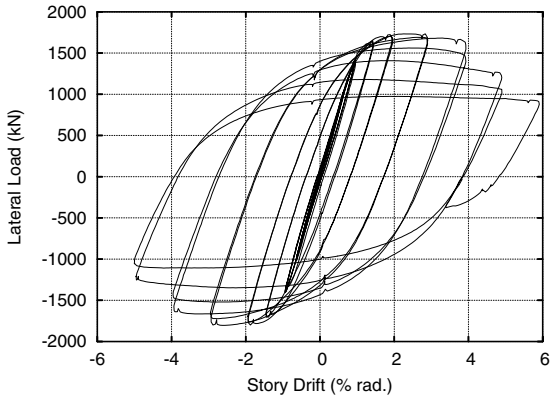

Figure 20. Lateral load-story drift hysteretic response of SPEC-4.

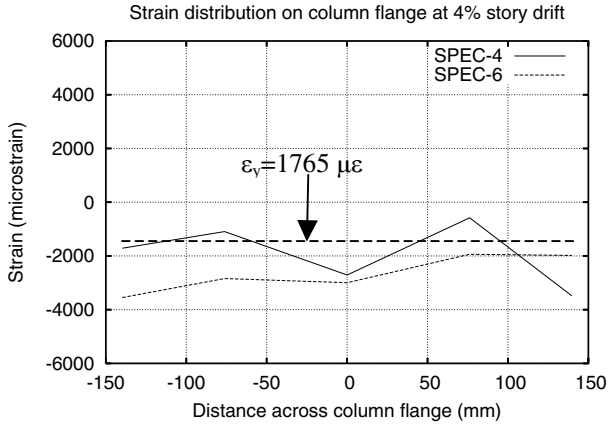

Figure 21. Longitudinal strain profile across column flange, just below RBS connection.

A summary of the maximum drift developed in each test specimen is given in Figure 22. These results are from the last cycle of each specimen prior to any fracture or strength deterioration to below 80% of the specimen nominal capacity. All specimens are shown to exceed 0.04 rads. of drift, which is the current criteria in Appendix S of the AISC Seismic Provisions [5] for qualifying a connection for seismic use. A summary of the column twist and lateral displacement of the bottom flange δ_{flg} of the beam at the RBS at 4% story drift is given in Table 2. An examination of the results indicates that column twist tends to increase when the elastic torsional stiffness of the column $K_{\phi,col}$ is reduced. However, for a smaller beam section size, the column twist is reduced, although the column torsional stiffness is smaller (e.g., SPEC-5). This phenomenon is associated with a smaller demand on the column when a smaller beam is used. The column twist is reduced significantly in specimens with a supplemental brace (SPEC-3 and SPEC-6). An examination of the measured specimen beam flange lateral displacement δ_{flg} in Table 2 shows these

results to be less than the value of $0.2b_f$, which is the value recommended by Chi and Uang [2] for determining the design torque applied to the column. Consequently, the use of the value of $0.2b_f$ for determining the design torsional loading on the column from the RBS will result in a larger column design torque. This is evident by comparing the column total normal stress at the connection based on Chi and Uang's recommendation with the measured specimen response. The criterion by Chi and Uang anticipates column flange yielding occurring in SPEC-2, 4, and 5 (see Figure 17). The strains measured in the column of these specimens indicated no yielding in SPEC-2 and 5, with some minor yielding occurring in SPEC-4 (a maximum strain of 2 to 4 times the yield strain developed).

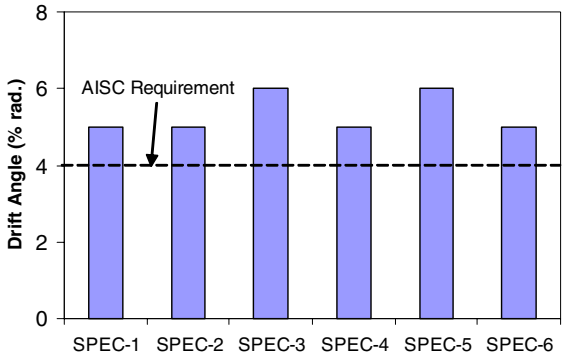

Figure 22. Specimen maximum drift achieved during tests.

SUMMARY AND CONCLUSIONS

An analytical and experimental program was conducted in order to evaluate the seismic performance of RBS connections to deep wide flange columns. The analytical study involved developing 3-D nonlinear finite element models and performing a parametric study to evaluate the effects of various parameters on connection performance. The results of the analytical study were used to develop a test matrix consisting of six full-scale specimens for the experimental program.

Based on the analytical study, the following main conclusions are noted:

1. RBS connections tend to have a reduced ductile fracture potential compared to a WUF connection due to the reduced amount of plastic strain developed in the former type of connection. Deeper columns do not necessarily result in a greater potential for ductile fracture in the connection. The ductile fracture potential and column twist in an RBS connection depends on the section modulus and torsional rigidity of the column section, where a greater amount of plastic strain and larger stresses in the column flange lead to a higher ductile fracture potential.
2. A weaker panel zone in a deep column RBS connection will not develop as much column twist as a connection with a stronger panel zone. However, a weaker panel zone can significantly increase the potential for ductile fracture of the connection. It is recommended that connections be designed with a balanced panel zone strength condition.
3. A composite floor slab can significantly reduce the lateral displacement of the beam bottom flange in the RBS and the amount of twist developed in the column. The slab appears to be effective in reducing the twist in deeper columns attached to an RBS connection, and enables the cyclic strength of the beam with an RBS connection to be better sustained. As a result, a larger amount of plastic strain develops in the connection when a composite floor slab is present, which increases the fracture potential of the RBS connection. The effect of beam-web slenderness is significantly reduced when a composite floor slab exists.

Based on the experimental study, the following main conclusions are noted:

1. All of the specimens were able to satisfy the criteria in the AISC Seismic Provisions [5] for qualifying the connection for seismic use.
2. A supplemental brace at the end of the RBS significantly reduced the transverse movement of the beam flanges in the RBS and column twist, and restrained the beam web and flanges against developing significant local buckling that leads to a cyclic degradation in specimen capacity.

3. Basing the column torque on a transverse movement of the beam flange in the RBS of $0.2b_f$ for calculating column flange warping stresses appears to be conservative. A new procedure for estimating the torsional load applied to the column due to the local and lateral buckling in the RBS is needed. Such a procedure is currently under development by the authors.

ACKNOWLEDGEMENTS

The research reported herein was supported by a grant from the American Institute of Steel Construction (Mr. Tom Schlafly program manager) and from the Pennsylvania Department of Community and Economic Development through the Pennsylvania Infrastructure Technology Alliance (PITA) program. The following companies donated materials for the experimental testing conducted in this research project: Arcelor International America of New York, NY (steel sections); Nucor Vulcraft Group of Chemung, NY (metal decking); and the Lincoln Electric Company of Cleveland, OH (welding wire). The support provided by the funding agencies and companies is greatly appreciated.

REFERENCES

1. Roeder, C. W. "Connection Performance State of Art Report," *Report No. FEMA-355D*, FEMA, Washington, D.C., 2000.
2. Chi, B. and Uang, C.-M. "Cyclic Response and Design Recommendations of Reduced Beam Section Moment Connections with Deep Columns," *Journal of Structural Engineering*, ASCE 2002, 128(4): 464-473.
3. Ricles, J., Zhang, X., Lu, L.W., and J. Fisher, "Development of Seismic Guidelines for Deep-Column Steel Moment Connections," American Institute of Steel Construction Research Report, November, 2003.
4. HKS *ABAQUS User's Manual*, Ver 6.1, Hibbit, Karlsson & Sorenson, Inc., Pawtucket, RI, 2001.
5. "*Seismic Provisions for Structural Steel Buildings*," American Institute of Steel Construction, Chicago, Illinois, 2002.
6. Lee, S., and Lu, L. "Cyclic Tests of Full-Scale Composite Joint Subassemblages," *Journal of Structural Engineering,* ASCE, 1989, 115 (8): 1977-1998.
7. Jones, S. L., Fry, G. T. and Engelhardt, M. D. "Experimental Evaluation of Cyclically Loaded Reduced Beam Section Moment Connections," *Journal of Structural Engineering*, ASCE, 2002, 128(4): 441-451.
8. Hancock, J.W. and MacKenzie, A.C. "On the Mechanisms of Ductile Failure in High-Strength Steels Subjected to Multi-Axial Stress-States," *J. Mech. Phys. Solids*, 1976, 24: 147-169.
9. Ricles, J. M., Mao, C., Lu, L.-W. and Fisher, J. W. "Development and Evaluation of Improved Details for Ductile Welded Unreinforced Flange Connections," *Report No. SAC/BD-00/24*, SAC Joint Venture, Sacramento, California, 2000.
10. "Manual of Steel Construction-Load and Resistance Factor Design," Third Ed., AISC, Chicago, Illinois, 2001.
11. Engelhardt, M. D. "The 1999 T. R. Higgins Lecture: Design of Reduced Beam Section Moment Connections," *Proceedings: 1999 North American Steel Construction Conference*, American Institute of Steel Construction, Toronto, Canada, pp. 1-1 to 1-29, May 1999.
12. "Recommended Specifications and Quality Assurance Guidelines for Steel Moment-Frame Construction for Seismic Applications," *Report No. FEMA 353*, Federal Emergency Management Agency, Washington D. C., July 2000.
13. "Structural Welding Code – Steel," *AWS D1.1/D1.1M:2002*, American Welding Society, Miami, Florida, 2002.
14. "Specification for Carbon Steel Electrodes for Flux Cored Arc Welding," *ANSI/AWS A5.20-95*, American Welding Society, Miami, Florida, 1995.